Bioscience, Biotechnology, and Biochemistry, 2014

CD36, but not GPR120, is required for efficient fatty acid utilization during endurance exercise

Mina Fujitani[1], Shigenobu Matsumura[1], Daisaku Masuda[2], Shizuya Yamashita[3], Tohru Fushiki[1] and Kazuo Inoue[1,*]

[1]*Laboratory of Nutrition Chemistry, Graduate School of Agriculture, Kyoto University, Sakyou-ku, Japan;*
[2]*Department of Cardiovascular Medicine, Osaka University Graduate School of Medicine, Suita, Japan;*
[3]*Department of Community Medicine, Osaka University Graduate School of Medicine, Suita, Japan*

Received April 14, 2014; accepted May 20, 2014
http://dx.doi.org/10.1080/09168451.2014.940835

Fatty acids (FA) are an important energy source during exercise. In addition to its role as an energy supply for skeletal muscle, FA may activate signaling pathways that regulate gene expression. FA translocase/cluster of differentiation 36 (CD36) and G protein-coupled receptor GPR120 are long-chain FA receptors. In this study, we investigated the impact of CD36 or GPR120 deletion on energy metabolism during exercise. CD36 has been reported to facilitate cellular transport and oxidation of FA during endurance exercise. We show that CD36 deletion decreased exogenous FA oxidation during exercise, using a combination of ^{13}C-labeled FA oxidation measurement and indirect calorimetry. In contrast, GPR120 deletion had no observable effect on energy metabolism during exercise. Our results further substantiate that CD36-mediated FA transport plays an essential role in efficient FA oxidation during exercise.

Key words: CD36; GPR120; endurance exercise; ^{13}C-labeled fatty acid oxidation measurement; indirect calorimetry

Energy substrates during exercise are determined by the intensity and duration of the exercise. The main fuel sources for endurance exercise are carbohydrates and fat. Prior fat utilization will spare glycogen stores and prevent hypoglycemia, and thus may be advantageous for endurance exercise. Non-esterified fatty acids (NEFAs) supplied via the bloodstream to contracting muscles are an important energy substrate for endurance exercise.[1–5] Furthermore, the concentration of NEFA in the blood increases during low–moderate exercise intensity and has also been suggested to be involved in activating signaling pathways that regulate gene expression in fat and carbohydrate metabolism.[6–8]

Fatty acid (FA) translocase, also known as cluster of differentiation 36 (CD36), is a multifunctional transmembrane glycoprotein that binds long-chain fatty acids (LCFAs) and facilitates their uptake into cells.[9] Recently, McFarlan et al. showed higher respiratory exchange ratio (RER) and lower FA transport in isolated skeletal muscle in CD36 knockout (CD36KO) mice than in wild-type (WT) mice during exercise, concluding that CD36 is a key component of the molecular machinery required for regulating skeletal muscle energy substrate utilization during exercise.[10] However, their data of respiratory gas analysis was just an average of exercise session and the time-course data of real-time changes in the whole animal with regard to carbohydrate, and fat oxidation of CD36KO mice has never been presented. Indirect calorimetry measurements may not provide an accurate measure of substrate oxidation under conditions when rates of gluconeogenesis, ketogenesis, or lipogenesis are elevated.[11] In actual exercise (under the changing circumstances depending on exercise duration), further detailed studies of the role of CD36 in NEFA uptake and utilization was required.

LCFA has been shown to activate the G protein-coupled receptor GPR120.[12] In recent years, the involvement of GPR120 in regulation of whole-body energy metabolism has been increasingly demonstrated. Deficiency of GPR120 alters the expression of genes regulating carbohydrate and fat metabolism, such as Scd1, Cd36, and insulin-signaling components, in adipose tissue and liver.[13] In addition, previous studies have reported that stimulation of GPR120 in 3T3-L1 adipocytes increased glucose transporter 4 (GLUT4) translocation to the cell surface,[14] and that GPR120 mRNA in skeletal and cardiac muscle was elevated in rats that fed a high-fat diet.[15] Thus, GPR120 is hypothesized to detect and respond to not only dietary FAs, but also to those increased by lipolysis during

*Corresponding author. Email: ashlaoh@kais.kyoto-u.ac.jp
Abbreviations: CD36, fatty acid translocase/cluster of differentiation 36; GPR120, G protein-coupled receptor 120; FA, fatty acid; LCFAs, long-chain fatty acids; NEFA, non-esterified fatty acid; TG, triglyceride; IMTG, intramuscular triglyceride; KO, knockout; WT, wild-type; RER, respiratory exchange ratio; VO_2, oxygen consumption; GLUT4, glucose transporter 4; Scd1, stearoyl-CoA desaturase 1.

exercise, thereby participating in the regulation of carbohydrate and fat metabolism.

CD36 is associated with LCFA-induced signal transduction in various cells as well as facilitation of LCFA uptake. Both CD36 and GPR120 can bind LCFA and function in the same direction via a distinct mechanism, as evidenced in studies reporting increases in free intracellular calcium concentrations in taste bud cells,[16] secretion of gut peptides from intestinal endocrine cells,[17,18] and adipocyte differentiation and lipogenesis,[19,20] whereas they exert opposite effects in other instances, such as pro-inflammatory CD36 effects in adipocytes and macrophages[21] and anti-inflammatory GPR120 effects in macrophages.[14] Accordingly, the present study aims to investigate the impact of CD36 and GPR120 deficiency in the regulation of whole-body energy metabolism during endurance exercise via comparison of CD36KO, GPR120 knockout (GPR120KO), and their corresponding WT littermates. In addition, the role of CD36 as a LCFA transporter in endurance exercise was further studied by estimating exogenous FA utilization in combination with measurement of ^{13}C-labeled substrate oxidation and indirect calorimetry in CD36KO and WT littermates. As ^{13}C is a stable isotope that makes up 1.115% of the carbon found in nature, the metabolic rate of ^{13}C-labeled substrates can be determined by measurement of the expiratory $^{13}CO_2/^{12}CO_2$ ratio. This method allows for the noninvasive monitoring of real-time changes in substrate oxidation in freely moving animals.[22,23]

Materials and methods

Animals. This study was approved by and conducted in accordance with the ethics guidelines of the Kyoto University Animal Experimentation Committee and in complete compliance with the National Institutes of Health Guide for the Care and Use of Laboratory Animals. CD36KO mice were maintained on a C57BL6/J background, kindly provided by Mason W. Freeman, MD, PhD, from Harvard Medical School.[24] GPR120KO mice on a BALB/c background were kindly provided by Dr Eguchi Ai of Kyoto University Graduate School of Agriculture. Mice were bred and housed under controlled temperature (22 °C) and lighting (12:12 h light–dark cycle) with free access to standard mouse chow (MF, Oriental Yeast, Tokyo, Japan) and water. Male KO mice and WT littermates (11–14 weeks old) were used throughout this study. All experiments were carried out during the daytime (8:00–18:00 h). To habituate mice to running on the treadmill, mice were run at 5–8 m/min (incline of 0°) for 10 min on the day before the experiment.

Genotyping. Genomic tail DNA samples were extracted using a nucleic acid extraction kit (Kurashiki Boseki, Kurashiki-shi, Japan). Genotyping was performed by PCR (GoTaq® Hot Start green Master Mix: Promega Corp., Madison, WI, USA) with cycle conditions of 94 °C for 30 s, 58 °C for 30 s, and 72 °C for 1 min for 38 cycles with a final extension of 5 min at 72 °C. PCR products were separated on a 2% agarose gel and visualized by SYBR Gold staining (SYBR® Gold Nucleic Acid Gel Stain, Invitrogen™, Life Technologies Corp., Carlsbad, CA, USA). PCR primers used to genotype CD36KO mice were as follows: 5′-AGCTCCAGCAATGAGCCCAC-3′ (forward, WT), 5′-TGGAAGGATTGGAGCTACGG-3′ (forward, KO), and 5′-CATACATTGCTGTTTATGCATGA-3′ (reverse, KO or WT) (Fig. 1(A)). PCR primers used to genotype GPR120KO mice were as follows: 5′-GCTCTTCTACGTGATGACAATGAG-3′ (forward, WT), 5′-GAAGGGTGAGAACAGAGTACCTACA-3′ (forward, KO), and 5′-CCACCCACGACCTATTATTGTTAC-3′ (reverse, KO or WT) (Fig. 1(B)).

Respiratory gas analysis. Respiratory gas analysis was performed using an open-circuit metabolic gas analysis system connected directly to a mass spectrometer (Arco2000; ArcoSystem, Chiba, Japan). Each mouse was placed in a metabolic chamber designed to measure respiratory gas, and measurements were recorded as described previously.[23] The running system was a modular enclosed metabolic treadmill apparatus for mice (Columbus Instruments, Columbus, OH) consisting of four running lanes of equal dimensions (305 × 51 × 44 mm), with each lane encased in a metabolic chamber with an inside volume of approximately 2000 cm^3. An electric fan was used to mix the air. The mice were allowed to remain sedentary in the treadmill chamber for 45 min before being subjected to running at 10 m/min (incline of 3°) for 30 min. A sedentary state analysis was carried out with metabolic chamber having an inside volume of approximately 1280 cm^3. To investigate the effect of fasting and of a novel environment, analyses began immediately after mice were held in a chamber without food and water.

Oxidation of exogenous lipid and glucose during exercise. Oxidation of exogenous FA and glucose were assessed based on $^{13}CO_2$ expiration in respiratory gas

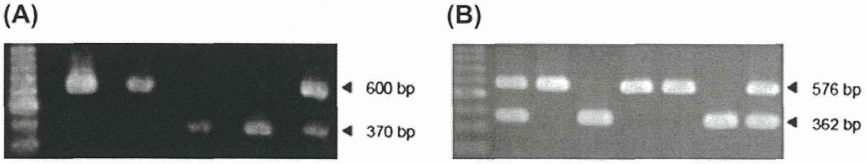

Fig. 1. Genotyping of mouse tail DNA by PCR.

Notes: (A) Agarose gel electrophoresis of SYBR gold-stained PCR products from CD36 knockout (370 bp band), WT (600 bp band), and heterozygous (2 bands; 370 and 600 bp) mice. (B) Agarose gel electrophoresis of SYBR gold-stained PCR products from GPR120 knockout (362 bp band), WT (576 bp band), and heterozygous (2 bands; 362 and 576 bp) mice.

after intragastric administration of ^{13}C-labeled palmitic acid or glucose.[22,23] ^{13}C-labeled palmitic acid (Isotec, Tokyo, Japan) solution containing 0.5% methylcellulose was intragastrically administered to mice 30 and 15 min before exercise at a concentration of 10 mM. ^{13}C-labeled glucose (Isotec, Tokyo, Japan) solution was intragastrically administered to mice 5 min before exercise at a concentration of 20 mM. The total amount of ^{13}C-labeled palmitic acid or glucose administered was 0.2 mmol/kg body weight, respectively.

Endurance test. Mice were exercised on a motorized treadmill (MK-680, Muromachi Kikai, Tokyo, Japan). An incremental protocol with increasing workloads was used (Fig. 3A). Four CD36KO mice and four WT mice were placed in individual treadmill lanes and ran in parallel. During the first 30 min, the speed was 10 m/min and increased 2 m/min every 30 min thereafter (incline of 3°). Exhaustion was defined as remaining on the shock electrode for more than 30 s.

Analysis of serum energy substrates. Blood samples were collected by decapitation. Mice were deprived of food for 60–90 min, and samples were collected at a sedentary state and just after treadmill running at 10 m/min (incline of 3°) for 30 min. Serum samples were isolated by centrifugation and stored at −70 °C until analysis. Serum glucose, lactate, NEFA, glycerol, beta-hydroxybutyric acid, and triglyceride (TG) levels were measured using appropriate assay kits (Glucose AR2: Wako Pure Chemical Industries, Ltd., Osaka, Japan; determiner LA: Kyowa Medex, Tokyo, Japan; NEFA C Test Wako: Wako Pure Chemical Industries; Glycerol Assay Kit: Funakoshi Co. Ltd., Tokyo, Japan; Ketone Test: Sanwa Chemical Institute, Nagoya, Japan; and TG E Test Wako: Wako Pure Chemical Industries).

Statistics. Data are expressed as the mean ± SEM. Data from respiratory gas analyses during exercise were analyzed by two-way repeated measures ANOVA and Student's *t*-test with Bonferroni corrections. Data from serum samples and endurance capacity were analyzed using an unpaired *t*-test. *p* values of 5% or less were considered statistically significant. Statistical analysis was conducted using the GraphPad Prism 5 software package (GraphPad, San Diego, CA, USA).

Results

RER and oxygen consumption during treadmill running and exercise performance

Respiratory exchange ratio (RER; Fig. 2(A) and (C)) and oxygen consumption (VO_2; Fig. 2(B) and (D))

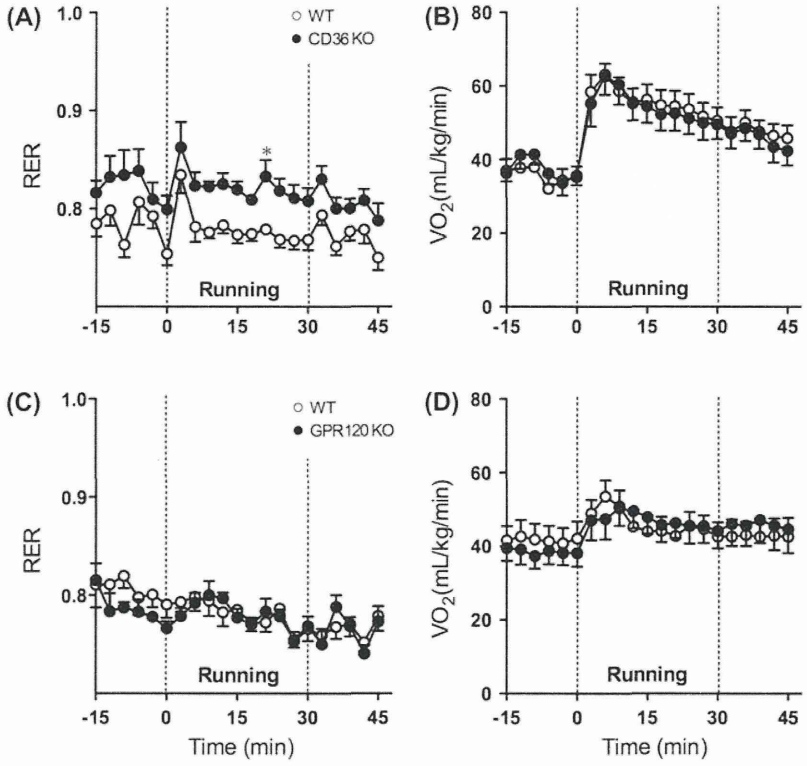

Fig. 2. Energy expenditure and substrate oxidation in CD36 and GPR120 knockout mice during exercise.

Notes: Time-course changes during treadmill running in respiratory exchange ratio (RER, A and C) and oxygen consumption (VO_2, B and D) were determined by respiratory gas analysis, and expressed as the means ± SEM at each time point. A and B, CD36 knockout (CD36KO) mice and WT littermates were forced to run on a treadmill at 10 m/min (incline of 3°) for 30 min ($n = 8$ for CD36KO; $n = 8$ for WT). *p* values were obtained by comparison of CD36KO and WT mice using two-way repeated measures ANOVA followed by Student's *t*-test with Bonferroni corrections. * $p < 0.05$ for CD36KO represents a significant difference versus WT littermates at each time point. C and D, GPR120 knockout (GPR120KO) mice and WT littermates were forced to run on a treadmill at 10 m/min (incline of 3°) for 30 min ($n = 6$ for GPR120KO; $n = 6$ for WT). *p* values were obtained by comparison of GPR120KO and WT mice using two-way repeated measures ANOVA followed by Student's *t*-test with Bonferroni corrections.

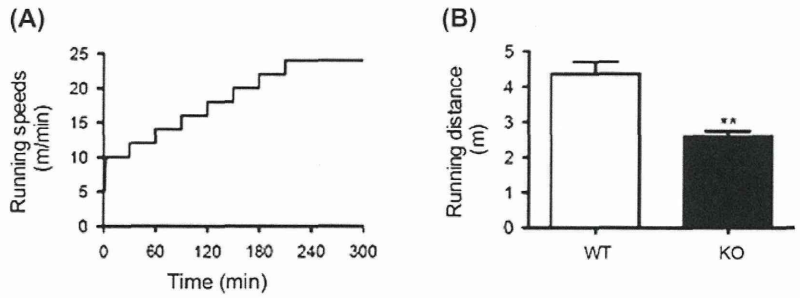

Fig. 3. Endurance capacity of CD36 knockout mice.

Notes: (A) Schematic representation of the treadmill protocol used for endurance exercise. (B) Running distance to fatigue of CD36 knockout (CD36KO) mice and WT littermates. Each value is the mean ± SEM ($n = 4$ for CD36KO; $n = 4$ for WT). p values were obtained by comparison of CD36KO and WT mice by Student's t-test. $^{**}p < 0.01$ for CD36KO represents a significant decrease versus WT littermates.

during treadmill running at 10 m/min (incline of 3°) for 30 min are shown in Fig. 2. Before running (from −15 to 0 min), RER tended to be higher in CD36KO mice than in WT mice but did not reach significance ($p = 0.0554$, 2-way repeated measures ANOVA). RER was higher in CD36KO mice compared with WT mice during exercise ($p < 0.01$, two-way repeated measures ANOVA during exercise; Fig. 2(A)). There was no difference in VO_2 between CD36KO and WT mice ($p > 0.05$, two-way repeated measures ANOVA before and during exercise; Fig. 2(B)). To investigate the running endurance capacity, an incremental protocol with increasing workloads was used (Fig. 3(A)), Running distance until exhaustion of CD36KO mice was significantly shorter than that of WT mice ($p < 0.01$, Student's t-test; Fig. 3(B)). There were no differences in RER and VO_2 between GPR120KO and WT mice ($p > 0.05$, two-way repeated measures ANOVA before and during exercise; Fig. 2(C) and (D)).

Exogenous FA and glucose as energy substrates during exercise

Exogenous FA oxidation during exercise was assessed through ^{13}C-labeled carbon dioxide excretion in respiratory gas after administration of ^{13}C-palmitic acids by stomach tube. $^{13}C/^{12}C$ (Fig. 4(A)), RER (Fig. 4(B)), and VO_2 (Fig. 4(C)) during treadmill

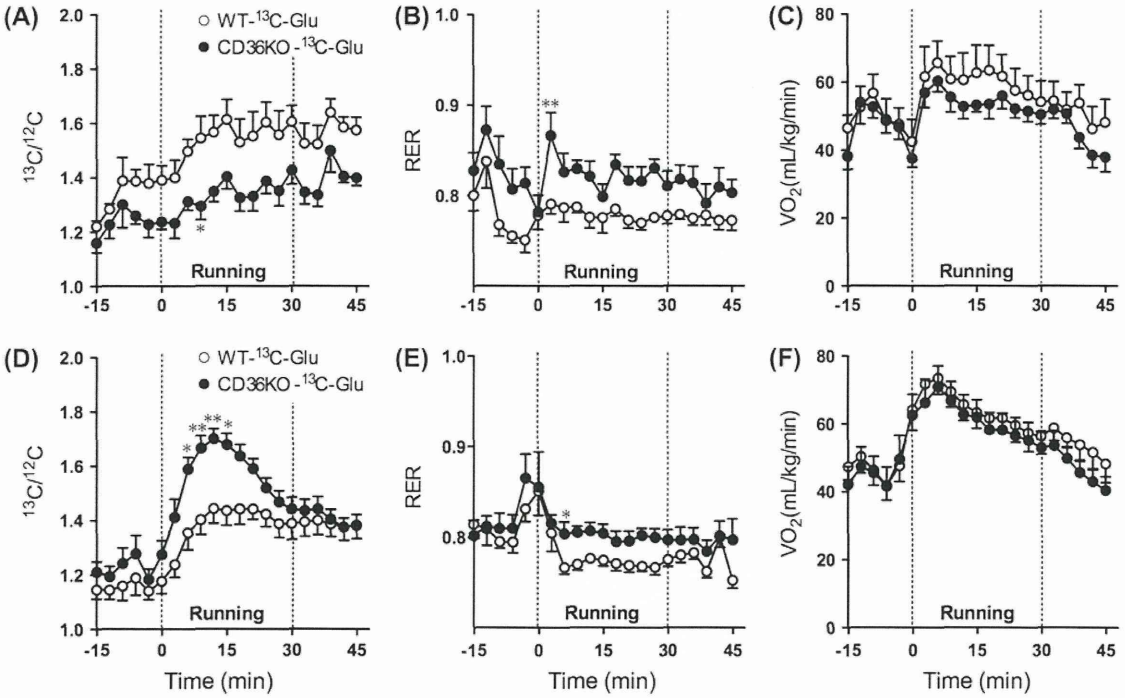

Fig. 4. Exogenous substrate oxidation in CD36 knockout mice during exercise.

Notes: Time-course changes during treadmill running in $^{13}C/^{12}C$ (A and D), respiratory exchange ratio (RER, B and E), and oxygen consumption (VO_2, C and F) were determined by respiratory gas analysis and ^{13}C-labeled fatty acid (FA) and glucose breath tests, and expressed as the means ± SEM at each time point. A, B, and C, Mice were administrated intragastrically with ^{13}C-labeled palmitic acid solution (^{13}C-PA) 30 and 15 min before forced treadmill running at 10 m/min (incline of 3°) for 30 min. The total amount of ^{13}C-labeled palmitic acid was 0.2 mmol/kg body weight ([($n = 7$ for CD36 knockout (CD36KO); $n = 6$ for WT]). D, E, and F, Mice were intragastrically administrated ^{13}C-labeled glucose solution (^{13}C-Glu) 5 min before forced treadmill running at 10 m/min (incline of 3°) for 30 min. The total amount of glucose administered was 0.2 mmol/kg body weight ($n = 8$ for CD36KO; $n = 7$ for WT). p values were obtained by comparison of CD36KO and WT mice using two-way repeated measures ANOVA followed by Student's t-test with Bonferroni corrections. $^{*}p < 0.05$ and $^{**}p < 0.01$ for CD36KO represents a significant difference versus WT littermates at each time point.

running at 10 m/min (incline of 3°) for 30 min are shown. During exercise, $^{13}C/^{12}C$ was significantly lower in CD36KO mice than in WT mice ($p < 0.05$, two-way repeated measures ANOVA during exercise; 9 min: $p < 0.05$, Student's *t*-test with Bonferroni corrections; Fig. 2(A)). RER was significantly higher in CD36KO mice than in WT mice ($p < 0.05$, two-way repeated measures ANOVA during exercise; 3 min: $p < 0.01$, Student's *t*-test with Bonferroni corrections; Fig. 4(B)), consistent with the changing patterns of $^{13}C/^{12}C$ during exercise. There was no difference in VO_2 between WT and CD36KO mice ($p = 0.3989$, two-way repeated measures ANOVA during exercise; Fig. 4(C)).

Exogenous glucose oxidation was also assessed during exercise. $^{13}C/^{12}C$ (Fig. 4(D)), RER (Fig. 4(E)), and VO_2 (Fig. 4(F)) during treadmill running at 10 m/min (incline of 3°) for 30 min are shown. During exercise, $^{13}C/^{12}C$ was significantly higher in CD36KO mice than in WT mice ($p < 0.05$, two-way repeated measures

Table 1. Serum energy substrates at sedentary state and during treadmill running.

	Sedentary		Exercise		2 way ANOVA		
	WT	CD36KO	WT	CD36KO	Interaction	Genotype	Exercise
Glucose (mg/dL)	178 ± 2	162 ± 3	168 ± 10	132 ± 7*	ns	$p < 0.05$	$p < 0.05$
LA[a] (mM)	0.82 ± 0.13	0.99 ± 0.15	0.53 ± 0.06	0.73 ± 0.19	ns	ns	ns
NEFA[b] (mEq/L)	0.61 ± 0.02	0.87 ± 0.05*	0.90 ± 0.04	1.25 ± 0.08***	ns	$p < 0.001$	$p < 0.001$
Glycerol (μM)	261 ± 25	254 ± 25	340 ± 9	360 ± 35	ns	ns	$p < 0.01$
BHBA[c] (mM)	134 ± 46	320 ± 67	382 ± 73	751 ± 94**	ns	$p < 0.01$	$p < 0.001$
TG[d] (mg/dL)	58.4 ± 9.9	65.5 ± 4.5	59.0 ± 5.6	55.4 ± 2.6	ns	ns	ns

Notes: Serum concentrations of glucose, lactic acid (LA), nonesterified fatty acid (NEFA), glycerol, beta-hydroxybutyric acid (BHBA), and triglyceride (TG) at sedentary state and immediately after treadmill running (10 m/min, incline 3°, 30 min) are shown. Blood samples were collected by decapitation. Mice were deprived of food for 60–90 min ($n = 5$ for CD36 knockout (CD36KO) at sedentary; $n = 5$ for CD36KO after exercise; $n = 4$ for WT at sedentary; $n = 6$ for WT after exercise). *p* values were obtained by comparison of CD36KO and WT mice using 2-way ANOVA followed by Student's *t*-test with Bonferroni corrections. *$p < 0.05$, **$p < 0.01$, and ***$p < 0.001$ for CD36KO represents significant differences versus WT littermates.

[a]lactic acid.

[b]nonesterified fatty acid.

[c]beta-hyderoxydutyric acid.

[d]triglyceride.

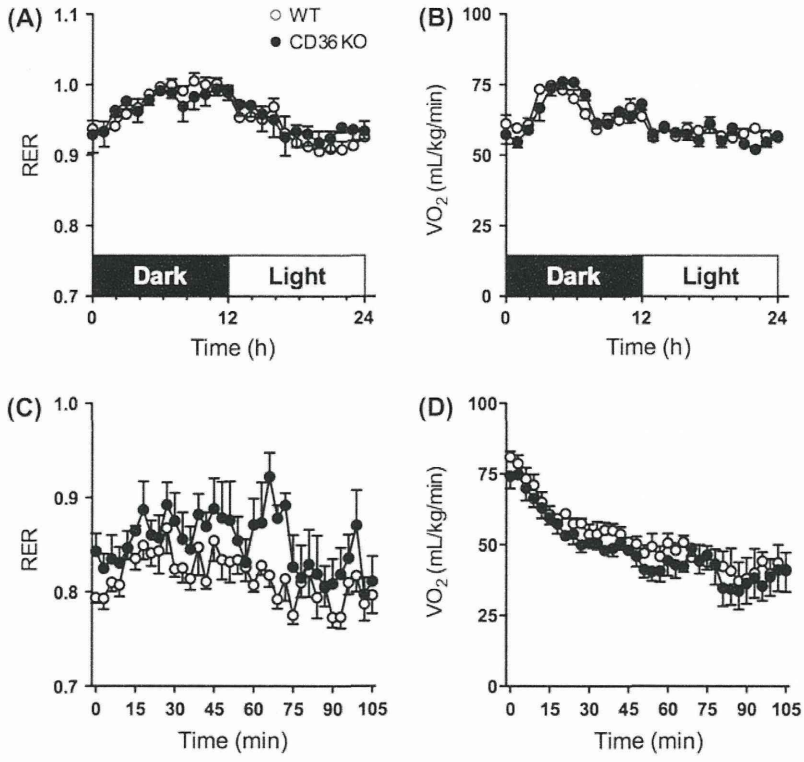

Fig. 5 Energy expenditure and substrate oxidation in CD36 knockout mice at rest.

Notes: (A) and (B), Diurnal changes in respiratory exchange ratio (RER, A) and oxygen consumption (VO_2, B) were determined by respiratory gas analysis and expressed as the means ± SEM at each time point. Mice were given food and water *ad libitum* and held individually in a chamber for 20 h before the expired air was analyzed ($n = 4$ for CD36 knockout (CD36KO); $n = 6$ for WT). C and D, RER (C) and VO_2 (D) were determined by respiratory gas analysis and expressed as the means ± SEM at each time point. The analyses began immediately after mice were held in a chamber without food and water ($n = 4$ for CD36KO; $n = 4$ for WT). *p* values were obtained by comparison of CD36KO and WT mice using two-way repeated measures ANOVA followed by Student's *t*-test with Bonferroni corrections.

ANOVA during exercise; 6 and 15 min: $p < 0.05$; 9–12 min: $p < 0.01$, Student's *t*-test with Bonferroni corrections; Fig. 4(D)). RER was significantly higher in CD36KO mice compared with WT mice ($p < 0.05$, two-way repeated measures ANOVA during exercise; 6 min: $p < 0.05$, by Student's *t*-test with Bonferroni corrections; Fig. 4(E)). There was no difference in VO_2 between WT and CD36KO mice ($p = 0.8202$, two-way repeated measures ANOVA during exercise; Fig. 4(F)).

Serum energy substrates before and during treadmill running

Serum concentrations of glucose, lactate, NEFA, glycerol, beta-hydroxybutyric acid, and TG before and after treadmill running (10 m/min, incline 3°, 30 min) are shown in Table 1. Serum glucose levels decreased, while NEFA, glycerol, and beta-hydroxybutyric acid levels increased after running compared with before running (glucose: $p < 0.05$; NEFA: $p < 0.001$; glycerol: $p < 0.01$; beta-hydroxybutyric acid: $p < 0.001$, two-way ANOVA; Table 1). Serum glucose levels after running were lower in CD36KO mice compared with WT mice ($p < 0.05$, by Student's *t*-test with Bonferroni corrections). The concentration of NEFA before and after running was higher in CD36KO mice compared with WT mice ($p < 0.001$, by Student's *t*-test with Bonferroni corrections). In contrast, there were no significant differences in glycerol levels before or after running between CD36KO and WT mice. Beta-hydroxybutyric acid levels after running were higher in CD36KO mice compared with WT mice ($p < 0.01$, by Student's *t*-test with Bonferroni corrections). There were no significant differences in the concentrations of lactate or TG before or after running between CD36KO and WT mice (two-way ANOVA; Table 1).

RER and oxygen consumption at a sedentary state

RER (Fig. 5(A)) and VO_2 (Fig. 5(B)) at sedentary state were not affected in CD36KO mice compared with WT mice over a 24 h time period (RER: $p = 0.6877$; VO_2: $p = 0.9784$, two-way repeated measures ANOVA). In a fasted state in a novel environment, RER tended to be higher in CD36KO mice than in WT mice but did not reach significance ($p = 0.1238$, two-way repeated measures ANOVA; Fig. 5(C)). There was no difference in VO_2 between WT and CD36KO mice ($p = 0.2909$, two-way repeated measures ANOVA; Fig. 5(D)).

Discussion

During endurance exercise, NEFA derived from lipolysis of adipose tissue triglyceride, intramuscular triglyceride (IMTG), triglyceride in the blood from chylomicrons, or from very low-density lipoprotein, is an important source of energy. A central role for CD36-mediated NEFA transport in regulating skeletal muscle FA oxidation during exercise and influencing aerobic exercise performance has been previously demonstrated by higher RER and lower FA transport in isolated skeletal muscle in CD36KO mice than in WT mice.[10] Further, in the present study, we provide more direct evidence in the whole animal that deficiency of CD36 leads to attenuated uptake and oxidation of NEFA and compensational strengthening of glucose utilization during actual exercise by directly evaluating the real-time changes of ^{13}C-labeled FA and glucose oxidation (Fig. 4(A) and (D)).[22,23] Primary energy sources utilized during exercise include skeletal muscle glycogen, IMTG, and extramuscular (blood-derived) glucose and NEFA.[1] CD36KO mice fed a chow diet had lower glycogen levels in the liver, heart, and muscle, lower TG levels in muscle and heart, and twofold higher TG levels in the liver compared with WT mice.[10,25] The current study further substantiates that deletion of CD36 affects whole-body fat utilization by not only changing the amount and distribution of energy sources but also by decreasing blood-derived NEFA uptake and oxidation during exercise. Correspondingly, McFarlan et al. reported that the increased NEFA transport rate in giant sarcolemmal vesicles derived from CD36KO mice was 1.7-fold lower than from WT mice after exercise.[10] However, the decreased exogenous FA oxidation observed in CD36KO mice could also be attributable to decreased intestinal FA absorption. When FA and TG were administered in the gastrointestinal tract, the rates of appearance in blood were similar between CD36KO and WT mice[26,27]; thus, we intragastrically administered ^{13}C-labeled FA to mice in this study. It has also been suggested that CD36 deficiency affects intestinal absorption of FA and chylomicron production,[28] and results were conflicting regarding secretion of intestine-derived lipoproteins into the mesenteric lymph.[29,30] Although the kinetics of intestine-derived FA in CD36-deficient animals are not yet completely understood, the above changes might contribute to the decreased exogenous FA oxidation during endurance exercise, though this possibility requires further investigation.

Our results showed that the increase in exogenous glucose oxidation in CD36KO mice was greater than in WT mice during exercise. The rate of muscle glycogen utilization and depletion of hepatic glycogen in CD36KO mice was reported to be higher than in WT mice.[10] These results demonstrate that CD36-mediated NEFA transport plays an essential role in efficient NEFA oxidation during endurance exercise, leading to sparing of carbohydrates that can be advantageous for prolonged endurance exercise.

Though CD36KO had no significant effect on sedentary energy metabolism, during *ad libitum* feeding, or in a habituated environment, it did result in a tendency towards higher RER than WT mice during food and water deprivation and in a novel environment. NEFA could be incorporated into cells by transporters other than CD36 (i.e. plasma membrane-associated fatty acid-binding protein or fatty acid transport proteins 1 and 4) or via passive diffusion;[9,31,32] however, during NEFA consumption conditions such as physical exercise, fasting, and in a novel environment, the effect of CD36 deficiency is likely not fully compensated by the other pathways.

Higher serum concentrations of NEFA and ketones (beta-hydroxybutyric acid) were observed after running in CD36KO mice, though glycerol concentration was

not different from WT mice (Table 1), and CD36KO lipolysis during treadmill running seemed similar to WT mice. With regards to serum ketone levels, CD36 is expressed in the liver at extremely low levels under normal conditions,[33] and a higher concentration of plasma ketone with increased NEFA influx to the liver of CD36KO mice has been reported.[34] In CD36KO mice, enhancement of lipolysis induced by running caused an increased influx of NEFA to the liver, resulting in higher ketone production. Contradictory to other studies,[25,26,34,35] serum TG levels were similar in both groups of mice before exercise under our experimental conditions (blood samples were collected after 1–1.5 h fasting during the light phase). Sandoval et al. also reported no significant difference in serum TG levels between CD36KO and WT mice after 12 h of food deprivation.[36] Several hypotheses were proposed, but the mechanism of hyperlipidemia in CD36KO mice has not been completely elucidated.[26,29,30]

No significant difference in blood glucose levels was observed between genotypes in sedentary conditions in this study, and similar results were observed in fed-state mice.[37] However, CD36KO mice showed significantly lower glucose levels compared with WT mice during exercise. Taken together with the higher exogenous glucose oxidation in CD36KO mice, the lower blood glucose in CD36KO mice is likely due to increased uptake and oxidation of blood glucose during exercise. Exercise-induced increased serum lactate levels were not observed in either genotype, suggesting that the exercise intensity was mild in this study.

We did not observe any effect of GPR120 deletion on energy metabolism during exercise (Fig. 2(C) and (D)). Although GPR120 functions as a receptor for LCFA,[12] it did not facilitate NEFA transport as an energy substrate distinct from CD36. However, previous studies have shown that GPR120 has a key role in sensing dietary fat, and consequently in the control of carbohydrate and fat metabolism.[13] Furthermore, stimulation of GPR120 with docosahexaenoic acid in 3T3-L1 adipocytes increased GLUT4 translocation to the cell surface with a subsequent increase in glucose transport into the cells.[14] Expression of GPR120 is very low and its function unclear in skeletal muscle, but GPR120 mRNA in cardiac tissue and extensor digitorum longus muscle were elevated in high-fat diet-fed rats.[15] It is conceivable that GPR120 not only detects dietary FAs, but also the increased NEFA derived from exercise-induced lipolysis, harmonizing the regulation of energy. Under conditions differing from the current study, energy metabolism during exercise may be affected by GPR120 deletion.

We investigated the impact of CD36 and GPR120 deletions on NEFA utilization during exercise. No effects of GPR120 deletion were observed on energy metabolism during exercise. However, CD36 deletion decreased whole-body exogenous FA oxidation and increased compensatory exogenous glucose oxidation. Our results provide evidence in the whole animal that CD36-mediated NEFA transport plays an essential role in efficient NEFA oxidation during exercise, which can be advantageous in endurance exercise.

References

[1] Romijn JA, Coyle EF, Sidossis LS, Gastaldelli A, Horowitz JF, Endert E, Wolfe RR. Regulation of endogenous fat and carbohydrate metabolism in relation to exercise intensity and duration. Am. J. Physiol. 1993;265:E380–E391.

[2] Hickson RC, Rennie MJ, Conlee RK, Winder WW, Holloszy JO. Effects of increased plasma fatty acids on glycogen utilization and endurance. J. Appl. Physiol. Respir. Environ. Exerc. Physiol. 1977;43:829–833.

[3] Fernandez C, Hansson O, Nevsten P, Holm C, Klint C. Hormone-sensitive lipase is necessary for normal mobilization of lipids during submaximal exercise. Am. J. Physiol. Endocrinol. Metab. 2008;295:E179–E186.

[4] Huijsman E, van de Par C, Economou C, van der Poel C, Lynch GS, Schoiswohl G, Haemmerle G, Zechner R, Watt MJ. Adipose triacylglycerol lipase deletion alters whole body energy metabolism and impairs exercise performance in mice. Am. J. Physiol. Endocrinol. Metab. 2009;297:E505–E513.

[5] Schoiswohl G, Schweiger M, Schreiber R, Gorkiewicz G, Preiss-Landl K, Taschler U, Zierler KA, Radner FP, Eichmann TO, Kienesberger PC, Eder S, Lass A, Haemmerle G, Alsted TJ, Kiens B, Hoefler G, Zechner R, Zimmermann R. Adipose triglyceride lipase plays a key role in the supply of the working muscle with fatty acids. J. Lipid Res. 2010;51:490–499.

[6] Tunstall RJ, Cameron-Smith D. Effect of elevated lipid concentrations on human skeletal muscle gene expression. Metabolism. 2005;54:952–959.

[7] Civitarese AE, Hesselink MK, Russell AP, Ravussin E, Schrauwen P. Glucose ingestion during exercise blunts exercise-induced gene expression of skeletal muscle fat oxidative genes. Am. J. Physiol. Endocrinol. Metab. 2005;289:E1023–E1029.

[8] Hoeks J, van Baak MA, Hesselink MK, Hul GB, Vidal H, Saris WH, Schrauwen P. Effect of beta1- and beta2-adrenergic stimulation on energy expenditure, substrate oxidation, and UCP3 expression in humans. Am. J. Physiol. Endocrinol. Metab. 2003;285: E775–E782.

[9] Schwenk RW, Holloway GP, Luiken JJ, Bonen A, Glatz JF. Fatty acid transport across the cell membrane: regulation by fatty acid transporters. Prostaglandins Leukot. Essent. Fatty Acids. 2010; 82:149–154.

[10] McFarlan JT, Yoshida Y, Jain SS, Han XX, Snook LA, Lally J, Smith BK, Glatz JF, Luiken JJ, Sayer RA, Tupling AR, Chabowski A, Holloway GP, Bonen A. In vivo, fatty acid translocase (CD36) critically regulates skeletal muscle fuel selection, exercise performance, and training-induced adaptation of fatty acid oxidation. J. Biol. Chem. 2012;287:23502–23516.

[11] Simonson DC, DeFronzo RA. Indirect calorimetry: methodological and interpretative problems. Am J Physiol. 1990;258: E399–E412.

[12] Hirasawa A, Tsumaya K, Awaji T, Katsuma S, Adachi T, Yamada M, Sugimoto Y, Miyazaki S, Tsujimoto G. Free fatty acids regulate gut incretin glucagon-like peptide-1 secretion through GPR120. Nat. Med. 2005;11:90–94.

[13] Ichimura A, Hirasawa A, Poulain-Godefroy O, Bonnefond A, Hara T, Yengo L, Kimura I, Leloire A, Liu N, Iida K, Choquet H, Besnard P, Lecoeur C, Vivequin S, Ayukawa K, Takeuchi M, Ozawa K, Tauber M, Maffeis C, Morandi A, Buzzetti R, Elliott P, Pouta A, Jarvelin MR, Körner A, Kiess W, Pigeyre M, Caiazzo R, Van Hul W, Van Gaal L, Horber F, Balkau B, Lévy-Marchal C, Rouskas K, Kouvatsi A, Hebebrand J, Hinney A, Scherag A, Pattou F, Meyre D, Koshimizu TA, Wolowczuk I, Tsujimoto G, Froguel P. Dysfunction of lipid sensor GPR120 leads to obesity in both mouse and human. Nature. 2012;483:350–354.

[14] Oh DY, Talukdar S, Bae EJ, Imamura T, Morinaga H, Fan W, Li P, Lu WJ, Watkins SM, Olefsky JM. GPR120 is an omega-3 fatty acid receptor mediating potent anti-inflammatory and insulin-sensitizing effects. Cell. 2010;142:687–698.

[15] Cornall LM, Mathai ML, Hryciw DH, McAinch AJ. Diet-induced obesity up-regulates the abundance of GPR43 and GPR120 in a tissue specific manner. Cell. Physiol. Biochem. 2011;28:949–958.

[16] Abdoul-Azize S, Selvakumar S, Sadou H, Besnard P, Khan NA. Ca^{2+} signaling in taste bud cells and spontaneous preference for fat: unresolved roles of CD36 and GPR120. Biochimie. 2014;96:8–13.

[17] Sundaresan S, Shahid R, Riehl TE, Chandra R, Nassir F, Stenson WF, Liddle RA, Abumrad NA. CD36-dependent signaling mediates fatty acid-induced gut release of secretin and cholecystokinin. FASEB J. 2013;27:1191–1202.

[18] Tanaka T, Katsuma S, Adachi T, Koshimizu TA, Hirasawa A, Tsujimoto G. Free fatty acids induce cholecystokinin secretion through GPR120. Naunyn Schmiedebergs Arch. Pharmacol. 2008;377:523–527.

[19] Christiaens V, Van Hul M, Lijnen HR, Scroyen I. CD36 promotes adipocyte differentiation and adipogenesis. Biochim. Biophys. Acta. 2012;1820:949–956.

[20] Gotoh C, Hong YH, Iga T, Hishikawa D, Suzuki Y, Song SH, Choi KC, Adachi T, Hirasawa A, Tsujimoto G, Sasaki S, Roh SG. The regulation of adipogenesis through GPR120. Biochem. Biophys. Res. Commun. 2007;354:591–597.

[21] Cai L, Wang Z, Ji A, Meyer JM, van der Westhuyzen DR. Scavenger receptor CD36 expression contributes to adipose tissue inflammation and cell death in diet-induced obesity. PLoS One. 2012;7:e36785.

[22] Ishihara K, Oyaizu S, Mizunoya W, Fukuchi Y, Yasumoto K, Fushiki T. Use of 13C-labeled glucose for measuring exogenous glucose oxidation in mice. Biosci. Biotechnol. Biochem. 2002;66: 426–429.

[23] Matsumura S, Saitou K, Miyaki T, Yoneda T, Mizushige T, Eguchi A, Shibakusa T, Manabe Y, Tsuzuki S, Inoue K, Fushiki T. Mercaptoacetate inhibition of fatty acid beta-oxidation attenuates the oral acceptance of fat in BALB/c mice. Am. J. Physiol. Regul. Integr. Comp. Physiol. 2008;295:R82–R91.

[24] Moore KJ, El Khoury J, Medeiros LA, Terada K, Geula C, Luster AD, Freeman MW. A CD36-initiated signaling cascade mediates inflammatory effects of beta-amyloid. J. Biol. Chem. 2002;277:47373–47379.

[25] Hajri T, Han XX, Bonen A, Abumrad NA. Defective fatty acid uptake modulates insulin responsiveness and metabolic responses to diet in CD36-null mice. J. Clin. Invest. 2002;109:1381–1389.

[26] Goudriaan JR, den Boer MA, Rensen PC, Febbraio M, Kuipers F, Romijn JA, Havekes LM, Voshol PJ. CD36 deficiency in mice impairs lipoprotein lipase-mediated triglyceride clearance. J. Lipid Res. 2005;46:2175–2181.

[27] Goudriaan JR, Dahlmans VE, Febbraio M, Teusink B, Romijn JA, Havekes LM, Voshol PJ. Intestinal lipid absorption is not affected in CD36 deficient mice. Mol. Cell. Biochem. 2002;239: 199–202.

[28] Abumrad NA, Davidson NO. Role of the gut in lipid homeostasis. Physiol. Rev. 2012;92:1061–1085.

[29] Masuda D, Hirano K, Oku H, Sandoval JC, Kawase R, Yuasa-Kawase M, Yamashita Y, Takada M, Tsubakio-Yamamoto K, Tochino Y, Koseki M, Matsuura F, Nishida M, Kawamoto T, Ishigami M, Hori M, Shimomura I, Yamashita S. Chylomicron remnants are increased in the postprandial state in CD36 deficiency. J. Lipid Res. 2009;50:999–1011.

[30] Drover VA, Ajmal M, Nassir F, Davidson NO, Nauli AM, Sahoo D, Tso P, Abumrad NA. CD36 deficiency impairs intestinal lipid secretion and clearance of chylomicrons from the blood. J. Clin. Invest. 2005;115:1290–1297.

[31] Nickerson JG, Alkhateeb H, Benton CR, Lally J, Nickerson J, Han XX, Wilson MH, Jain SS, Snook LA, Glatz JF, Chabowski A, Luiken JJ, Bonen A. Greater transport efficiencies of the membrane fatty acid transporters FAT/CD36 and FATP4 compared with FABPpm and FATP1 and differential effects on fatty acid esterification and oxidation in rat skeletal muscle. J. Biol. Chem. 2009;284:16522–16530.

[32] Jain SS, Chabowski A, Snook LA, Schwenk RW, Glatz JF, Luiken JJ, Bonen A. Additive effects of insulin and muscle contraction on fatty acid transport and fatty acid transporters, FAT/CD36, FABPpm, FATP1, 4 and 6. FEBS Lett. 2009;583: 2294–2300.

[33] Abumrad NA, el-Maghrabi MR, Amri EZ, Lopez E, Grimaldi PA. Cloning of a rat adipocyte membrane protein implicated in binding or transport of long-chain fatty acids that is induced during preadipocyte differentiation. Homology with human CD36. J. Biol. Chem. 1993;268:17665–17668.

[34] Goudriaan JR, Dahlmans VE, Teusink B, Ouwens DM, Febbraio M, Maassen JA, Romijn JA, Havekes LM, Voshol PJ. CD36 deficiency increases insulin sensitivity in muscle, but induces insulin resistance in the liver in mice. J. Lipid Res. 2003;44: 2270–2277.

[35] Febbraio M, Abumrad NA, Hajjar DP, Sharma K, Cheng W, Pearce SF, Silverstein RL. A null mutation in murine CD36 reveals an important role in fatty acid and lipoprotein metabolism. J. Biol. Chem. 1999;274:19055–19062.

[36] Sandoval JC, Nakagawa-Toyama Y, Masuda D, Tochino Y, Nakaoka H, Kawase R, Yuasa-Kawase M, Nakatani K, Inagaki M, Tsubakio-Yamamoto K, Ohama T, Nishida M, Ishigami M, Komuro I, Yamashita S. Fenofibrate reduces postprandial hypertriglyceridemia in CD36 knockout mice. J. Atheroscler. Thromb. 2010;17:610–618.

[37] Bonen A, Han XX, Habets DD, Febbraio M, Glatz JF, Luiken JJ. A null mutation in skeletal muscle FAT/CD36 reveals its essential role in insulin- and AICAR-stimulated fatty acid metabolism. Am. J. Physiol. Endocrinol. Metab. 2007;292: E1740–E1749.

OPEN

IDEAS AND INNOVATIONS
Breast

DIEP Flap Breast Reconstruction Using 3-dimensional Surface Imaging and a Printed Mold

Koichi Tomita, MD, PhD
Kenji Yano, MD, PhD
Yuki Hata, MD
Akimitsu Nishibayashi, MD
Ko Hosokawa, MD, PhD

Summary: Recent advances in 3-dimensional (3D) surface imaging technologies allow for digital quantification of complex breast tissue. We performed 11 unilateral breast reconstructions with deep inferior epigastric artery perforator (DIEP) flaps (5 immediate, 6 delayed) using 3D surface imaging for easier surgery planning and 3D-printed molds for shaping the breast neoparenchyma. A single- or double-pedicle flap was preoperatively planned according to the estimated tissue volume required and estimated total flap volume. The DIEP flap was then intraoperatively shaped with a 3D-printed mold that was based on a horizontally inverted shape of the contralateral breast. Cosmetic outcomes were assessed as satisfactory, as confirmed by the postoperative 3D measurements of bilateral breasts. We believe that DIEP flap reconstruction assisted with 3D surface imaging and a 3D-printed mold is a simple and quick method for rebuilding a symmetric breast. *(Plast Reconstr Surg Glob Open 2015;3:e316; doi: 10.1097/GOX.0000000000000288; Published online 5 March 2015)*

The deep inferior epigastric artery perforator (DIEP) flap is widely used in autologous tissue breast reconstruction because it offers a large volume of soft tissue without sacrificing the rectus muscle, with fewer complications such as hernia or bulge formation.[1,2] To optimize cosmetic outcomes in unilateral DIEP flap breast reconstruction, an adequate volume of flap tissue with good blood flow should be prepared and molded into a shape similar to the contralateral breast. For an inexperienced surgeon, however, surgery planning (eg, single- or double-pedicle) and intraoperative breast shaping can be difficult.

From the Department of Plastic and Reconstructive Surgery, Graduate School of Medicine, Osaka University, Osaka, Japan.
Received for publication November 18, 2014; accepted January 27, 2015.

DOI: 10.1097/GOX.0000000000000288

Recent advances in 3-dimensional (3D) body surface imaging enable us to digitally quantify complex breast regions noninvasively.[3,4] Models built with a personal 3D printer have also been used to aid various reconstructive surgeries.[5,6] We recently used these technologies, and in this report, we document our experiences with unilateral DIEP flap breast reconstruction with 3D surface imaging to improve surgery planning and 3D-printed molds to shape a breast symmetrical to the contralateral breast.

PATIENTS AND METHODS

Between April and October 2014, unilateral breast reconstruction with a DIEP flap was performed in 11 breast cancer patients at the Osaka University Hospital. The mean age of the patients was 50.7 years (range, 41–63 years), and the mean follow-up was 5 months (range, 3–8 months). Four cases were immediate reconstructions (after skin-sparing mastectomy), 1 was a delayed-immediate reconstruction, and 6 were 2-stage delayed reconstructions. This study

Disclosure: *The authors have no financial interest to declare in relation to the content of this article. The Article Processing Charge was paid for by a grant from the Japanese Ministry of Education, Science, Sports and Culture (25462789).*

was approved by our institutional review board, and appropriate informed consent was obtained from the patients.

3D Measurement of Breast Region and Estimation of Required Flap Volume

3D surface imaging of the bilateral breast region was performed in a sitting position with the David Structured Light Scanner SLS-1 (David Vision Systems GmbH, Koblenz, Germany) according to manufacturer's instructions. Typically, 2 prepared single shots were combined into one 3D image. Analysis was then performed with 3D image data analysis software developed for breast reconstruction (Breast-Rugle, Medic Engineering, Kyoto, Japan), and breast volume was estimated bilaterally (Fig. 1A). Estimated required flap volume was based on contralateral breast volume for 1-stage reconstruction or the volume difference between both sides for 2-stage reconstruction.

In 2-stage reconstruction, an anatomical integrated port tissue expander (Natrelle133, Allergan, Tokyo, Japan) was inserted subcutaneously in patients with no radiotherapy history or subpectorally in patients with radiotherapy before reconstruction. Final expansion volume was determined by estimated required flap volume and shape of the contralateral breast.

Estimation of Total Flap Volume and Determination of Flap Type

The total volume of DIEP flap can be precisely estimated by abdominal multidetector-row computed tomography and 3D imaging software.[7] However, total flap volume can also be estimated with the following formula: total flap volume (ml) = total flap area (cm^2) × mean subcutaneous fat thickness (cm). Total flap area was calculated using a preoperative abdominal photograph (Fig. 1B) and public domain image software (ImageJ, Wayne Rasband, National Institute of Health, Bethesda, Md.)). Mean subcutaneous fat thickness was determined by ultrasonic evaluation of subcutaneous fat at the upper and lower borders of the flap (Fig. 1B). Flap type was determined by dividing required flap volume by total flap volume, with a value greater than 0.6–0.7 (depending on size, number, and location of perforators[8,9]) necessitating a double-pedicle DIEP flap (ie, bilateral deep inferior epigastric vessels are used) (Fig. 1C).

Breast Mold Creation and Breast Mound Shaping

Using the Breast-Rugle software, contralateral breast data were horizontally inverted to generate breast mold data. An acrylonitrile–butadiene–styrene copolymer breast mold was then created with a personal 3D printer (MakerBot Replicator 2x, MakerBot

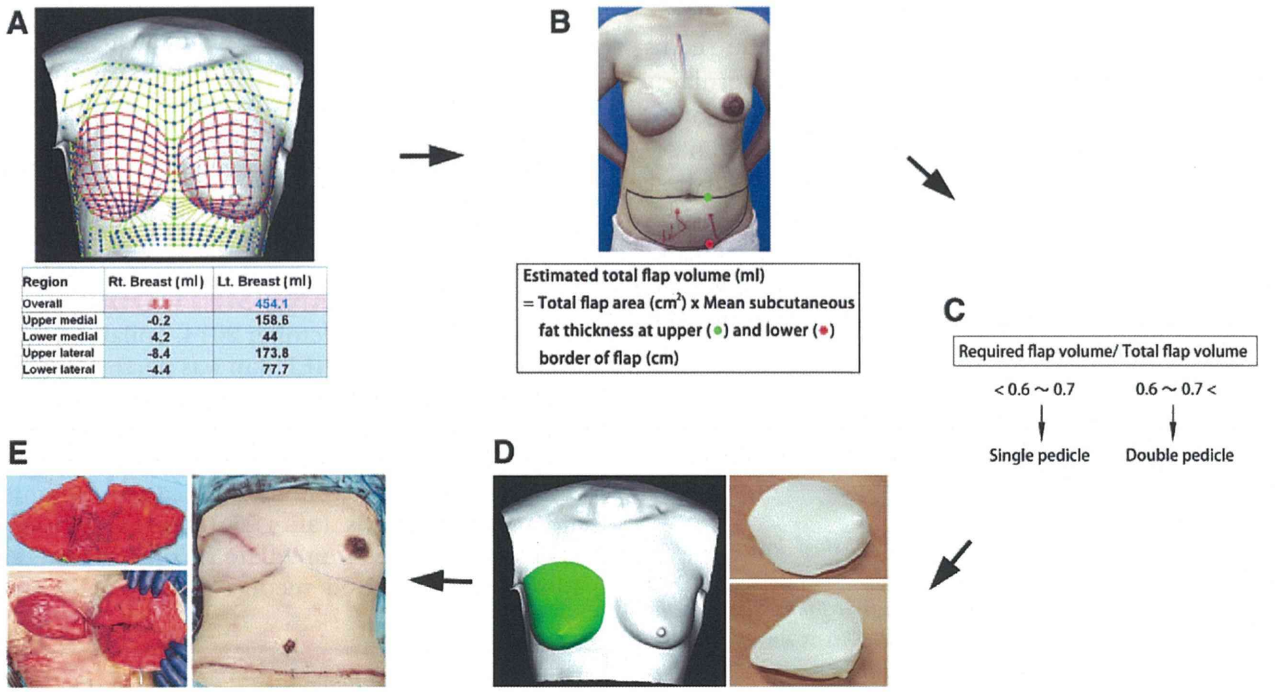

Fig. 1. Workflow images of DIEP flap breast reconstruction assisted with 3D surface imaging. A, Required flap volume was estimated from bilateral breast images using 3D image data analysis software. B and C, Total flap volume was estimated using the formula shown, and flap type was determined preoperatively. D, Contralateral breast shape was horizontally inverted, and an acrylonitrile–butadiene–styrene copolymer breast mold was created using a personal 3D printer. E, After vascular anastomosis, the de-epithelialized flap was placed in the mold and fixed to shape a symmetric breast.